

Transmission-electron microscopy study of the shape of buried $\text{In}_x\text{Ga}_{1-x}\text{As}/\text{GaAs}$ quantum dots

X. Z. Liao,* J. Zou, X. F. Duan,[†] and D. J. H. Cockayne

Australian Key Centre for Microscopy and Microanalysis, The University of Sydney, Sydney, NSW 2006, Australia

R. Leon[‡] and C. Lobo

Department of Electronic Materials Engineering, Research School of Physical Sciences and Engineering, Australian National University, Canberra ACT 0200, Australia

(Received 27 April 1998)

High-resolution electron microscopy, on-zone bright-field imaging, and image simulation were used to investigate the shape of capped $\text{In}_{0.6}\text{Ga}_{0.4}\text{As}/\text{GaAs}$ semiconductor quantum dots. Cross-section $\langle 110 \rangle$ high-resolution images suggest that the quantum dots are lens shaped, while the $[001]$ on-zone bright-field images show a contrast that suggests a quantum dot morphology with four edges parallel to $\langle 100 \rangle$. The image simulation, however, suggests that a spherical quantum dot can produce a square-shaped image. These observations lead to the conclusion that the quantum dots in buried $\text{In}_{0.6}\text{Ga}_{0.4}\text{As}/\text{GaAs}$ semiconductor heterostructures are lens shaped. [S0163-1829(98)51432-4]

Quantum dots in semiconductors have important potential applications in optoelectronic devices.¹ Carriers in quantum dots are confined three dimensionally, so that the optoelectronic properties are different from those in bulk materials, quantum wells, and quantum wires. The shape and size of quantum dots are important parameters in determining their optoelectronic properties.²⁻⁵ The most frequently used techniques to study their shape and size are atomic force microscopy (AFM),⁶⁻¹¹ scanning tunneling microscopy (STM),^{12,13} reflection high-energy electron diffraction (RHEED),^{14,15} and transmission-electron microscopy (TEM).^{1,12,16-18} Different shapes of quantum dots such as lens shaped or round shaped,⁷⁻¹⁹ pyramids with different facets,^{9,10,13-17} and truncated pyramids^{1,18} have been reported using the above techniques.

Differences in the calculated values for quantum dot ground-state and excited-state emission, and in intersublevel energies will be obtained depending on what shapes and aspect ratios are assumed in the calculation. Calculations for both pyramid-shaped²⁰ and lens-shaped $\text{In}_x\text{Ga}_{1-x}\text{As}/\text{GaAs}$ quantum dots²¹ have been reported; however, an exact ex-

perimental determination of the shape of these islands is at present controversial.

It is well known that AFM and STM can only be used to study quantum dots on the top surface⁶⁻¹² or cross-section specimens of buried quantum dots where the dots are exposed on the specimen's surface.¹³ However, these techniques are inappropriate and not useful for studying the morphology of buried quantum dots. RHEED is also a surface technique, but since it is an indirect method, its results can easily be misinterpreted.¹⁴ TEM is the only tool capable of studying buried quantum dots. However, under the usual dynamical two-beam imaging or on-zone axis multibeam imaging conditions, the diffraction contrast image is formed largely by the strain field around the quantum dots, rather than by their shape and size directly. As a result, it is not possible to interpret diffraction contrast images without image simulations.^{22,23} In this paper, we determine the shape of buried quantum dots in $\text{In}_{0.6}\text{Ga}_{0.4}\text{As}/\text{GaAs}$ strained-layer heterostructures by high-resolution electron microscopy (HREM), and by on-zone bright-field imaging with image simulation.

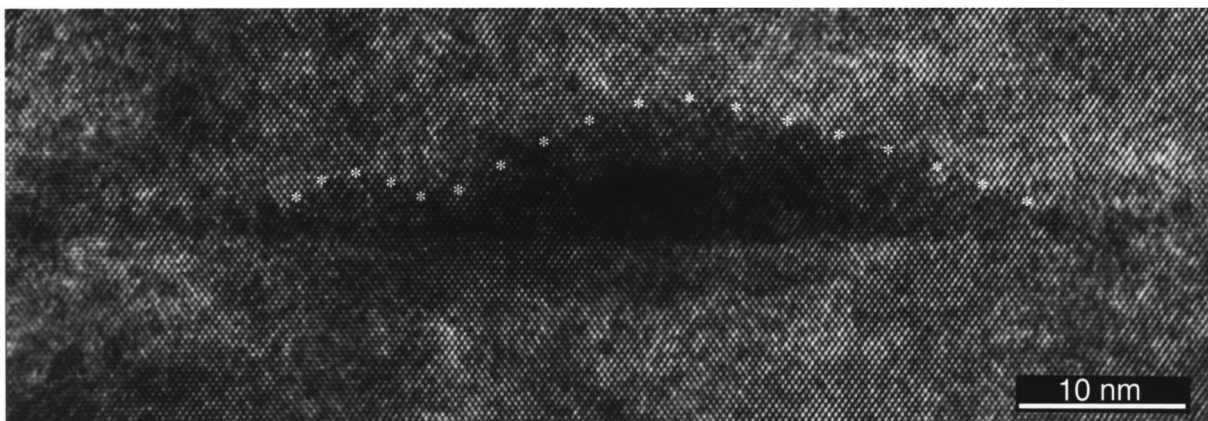


FIG. 1. A $\langle 110 \rangle$ cross-section HREM image of buried $\text{In}_{0.6}\text{Ga}_{0.4}\text{As}$ quantum dots showing two lens-shaped dots partially overlapped. The boundaries are highlighted using white stars.

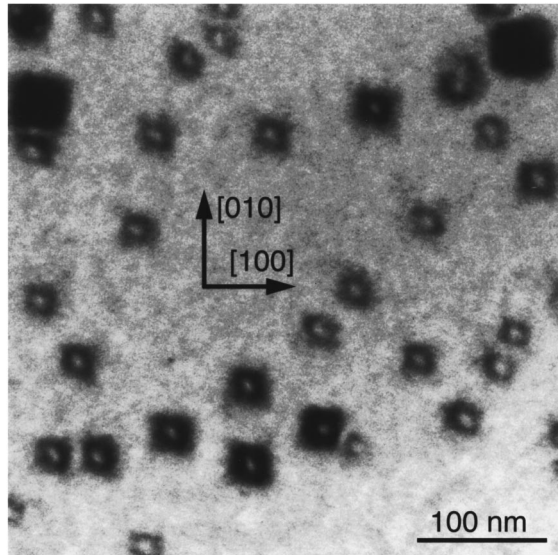


FIG. 2. A [001] on-zone bright-field image of buried $\text{In}_{0.6}\text{Ga}_{0.4}\text{As}$ quantum dots showing square-shaped contrast with edges parallel to $\langle 100 \rangle$.

Capped nm-size $\text{In}_{0.6}\text{Ga}_{0.4}\text{As}$ quantum dots were grown by metalorganic chemical vapor deposition using a horizontal reactor cell operating at 76 Torr on a (001) GaAs substrate. The growth temperature during the island growth was 550 °C. An 80-nm-thick capping layer of GaAs was grown on top of the dots while ramping the growth temperature to 650 °C. Further details of the growth procedure are reported elsewhere.^{24,25}

Plan-view and $\langle 110 \rangle$ cross-section TEM specimens were prepared by ion-beam thinning using a Gatan 660 Ion-Beam Thinner with a cold stage to prevent preferred thinning. TEM investigations were performed in Philips EM430, Philips CM12, and Philips FEG CM200 transmission electron microscopes.

To determine the shape of GaAs capped $\text{In}_{0.6}\text{Ga}_{0.4}\text{As}$ quantum dots grown on an (001) GaAs substrate, a HREM

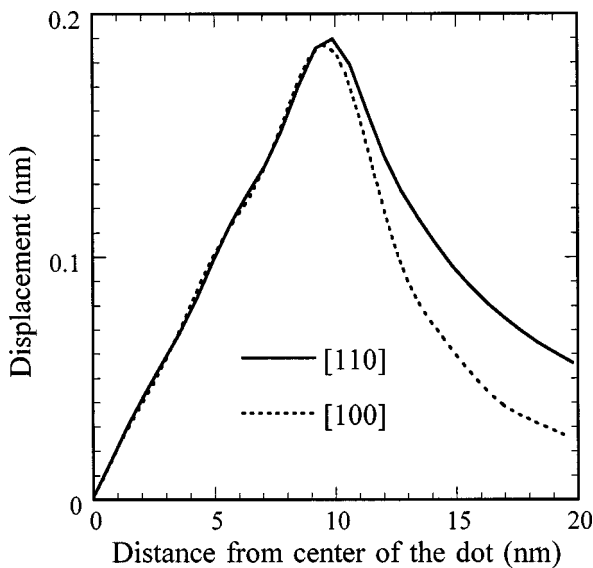


FIG. 3. Total displacement as a function of distance from the center of a dot, along [100] and [110] directions, respectively.

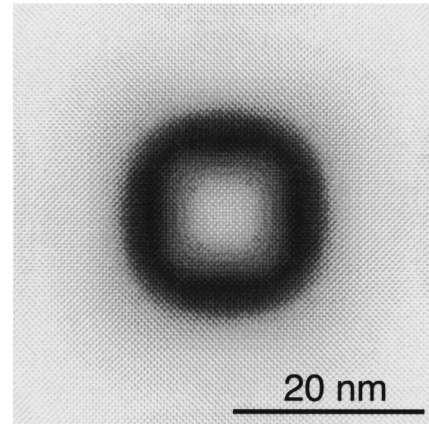


FIG. 4. A simulated [001] on-zone bright-field image of a buried spherical dot showing a near square contrast with edges parallel to $\langle 100 \rangle$. The following parameters are used in the image simulation: accelerating voltage, 120 kV; number of electron beams used in the simulation, 29; film thickness, 80 nm; depth of dot center in the sample, 40 nm; dot radius, 10 nm; and lattice mismatch, 3.6%.

study of $\langle 110 \rangle$ cross-section samples of buried quantum dots was carried out. Figure 1 is a typical cross-section HREM image, showing large and small lens-shaped $\text{In}_{0.6}\text{Ga}_{0.4}\text{As}$ quantum dots, partially overlapped. The aspect ratio of height to diameter is approximately 1:5 for the large dot and approximately 1:4 for the small dot, while the diameter of the large dot is around 42 nm. Images from other dots have aspect ratios between these values, which is in agreement with the values measured by AFM and cross-section HREM for uncapped quantum dots.^{11,12,17} This agreement suggests that there is no shape change during the growth of the capping layer, even though such a change has been suggested.^{26,27}

While the HREM images suggest that the quantum dots are lens shaped, [001] on-zone bright-field images suggest otherwise. As shown in Fig. 2, the images of many quantum dots are seen, with square shapes, and edges parallel to $\langle 100 \rangle$. The edge lengths vary between 20 and 40 nm. Ruvimov *et al.*¹⁶ have reported a similar square-shaped diffraction contrast image, which, combined with their cross section HREM image, led them to conclude that their quantum dots were of pyramid shape with a square base. However, from our image simulations below, we argue that extreme caution is required in interpreting the shape of quantum dots from the shape of on-zone experimental images, and we believe that the same caution is also needed in interpreting the images of Ruvimov *et al.*¹⁶

To investigate the relationship between the image symmetry and the shape of quantum dots, image simulations were carried out using multibeam dynamical electron scattering theory,²⁸ with the strain field introduced as a local displacement $R_{(x,y,z)}$. As $R_{(x,y,z)}$ is not easily obtained for a lens-shaped quantum dot, a spherical quantum dot was used, having the same radial symmetry as the lens-shaped dot when observed from [001], as in the experiment. The formulation of Mura²⁹ was used for determining this displacement, with the anisotropic elastic constants c_{11} , c_{12} , and c_{44} of $\text{In}_{0.6}\text{Ga}_{0.4}\text{As}$ set equal to those of GaAs.³⁰ This formulation

assumes a periodic array (in three dimensions) of dots. Provided that the dot spacing is not too small, this periodicity does not affect the displacement field significantly, although it does affect the calculation speed. A periodicity of eight times the dot diameter was chosen, following the work of Degischer³¹ that suggests that this spacing is sufficiently large for that purpose. For simplicity, the structure factors of GaAs and $\text{In}_{0.6}\text{Ga}_{0.4}\text{As}$ were assumed to be equal.

Figure 3 shows calculated displacement fields along [100] and [110] for a spherical dot with a radius of 10 nm. It is clear that the displacement field is different along the two directions because of the symmetry of the cubic lattice, and in fact, it has fourfold symmetry along [001]. Such a difference will certainly affect diffraction contrast images.

Figure 4 shows a simulated [001] on-zone bright-field image of the spherical model $\text{In}_{0.6}\text{Ga}_{0.4}\text{As}$ quantum dot inside the GaAs. The simulated image has a near square shape with edges parallel to $\langle 100 \rangle$, even though the dot is spherical in shape. This simulated image is in excellent agreement with images obtained experimentally, as shown in Fig. 2. Mat-

sumura *et al.*²³ also reported experimental and simulated fourfold symmetry in [001] on-zone bright-field images from spherical Co-rich precipitates in a Cu-Co matrix. From this we conclude that buried spherical quantum dots in the cubic lattices can appear having fourfold symmetry in $\langle 001 \rangle$ on-zone bright-field images.

It is clear from these image simulations that the on-zone bright-field image contrast of quantum dots will reflect the symmetry of the lattice rather than the symmetry of the quantum dot. Furthermore, we conclude that a lens-shaped quantum dot viewed along [001] will show fourfold symmetry. From this, we conclude that the image of Fig. 2 could arise from lens-shaped quantum dots, in agreement with the shape determined from HREM.

The authors would like to thank the Australian Research Council for financial support, Professor S. Matsumura of Kyushu University for providing the simulation program, and Dr. G. Anstis of the University of Technology, Sydney, for assistance with programming.

*Electronic address: xzliao@emu.usyd.edu.au

[†]On leave from Beijing Laboratory of Electron Microscopy, P.O. Box 2724, Beijing 100080, P. R. China.

[‡]Present address: Jet Propulsion Laboratory, California Institute of Technology, 4800 Oak Grove Drive, Pasadena, California 91109-8099.

¹K. Eberl, *Phys. World* **10**, 47 (1997).

²H. Jiang and J. Singh, *Phys. Rev. B* **56**, 4696 (1997).

³R. Leon, S. Fafard, D. Leonard, J. L. Merz, and P. M. Petroff, *Appl. Phys. Lett.* **67**, 521 (1995).

⁴A. A. Seraphin, E. Werwa, and K. D. Kolenbrander, *J. Mater. Res.* **12**, 3386 (1997).

⁵J. L. Zhu, Z. Q. Li, J. Z. Yu, K. Ohno, and Y. Kawazoe, *Phys. Rev. B* **55**, 15 819 (1997).

⁶C. Lobo and R. Leon, *J. Appl. Phys.* **83**, 4168 (1998).

⁷J. M. Moison, F. Houzay, F. Barthe, L. Leprince, E. Andre, and O. Vatel, *Appl. Phys. Lett.* **64**, 196 (1994).

⁸J. H. Zhu, K. Brunner, and G. Abstreiter, *Appl. Phys. Lett.* **72**, 424 (1998).

⁹H. Saito, K. Nishi, S. Sugou, and Y. Sugimoto, *Appl. Phys. Lett.* **71**, 590 (1997).

¹⁰Z. Zhu, E. Kurtz, K. Arai, Y. F. Chen, D. M. Bagnall, P. Tomashini, F. Lu, T. Sekiguchi, T. Yao, T. Yasuda, and Y. Segawa, *Phys. Status Solidi B* **202**, 827 (1997).

¹¹D. Hommel, K. Leonardi, H. Heinke, H. Selke, K. Ohkawa, F. Gindele, and U. Woggon, *Phys. Status Solidi B* **202**, 835 (1997).

¹²Y.-W. Mo, D. E. Savage, B. S. Swartzentruber, and M. G. Lagally, *Phys. Rev. Lett.* **65**, 1020 (1990).

¹³W. Wu, J. R. Tucker, G. S. Solomon, and J. S. Harris, Jr., *Appl. Phys. Lett.* **71**, 1083 (1997).

¹⁴H. Lee, R. Lowe-Webb, W. Yang, and P. C. Sercel, *Appl. Phys. Lett.* **72**, 812 (1998).

¹⁵Y. Nabetani, T. Ishikawa, S. Noda, and A. Sasaki, *J. Appl. Phys.* **76**, 347 (1994).

¹⁶S. Ruvimov, P. Werner, K. Scheerschmidt, U. Gosele, J. Heydenreich, U. Richter, N. N. Ledentsov, M. Grundmann, D. Bimberg, V. M. Ustinov, A. Yu. Egorov, P. S. Kop'ev, and Z. I. Alferov, *Phys. Rev. B* **51**, 14 766 (1995).

¹⁷K. Tillmann, A. Thust, M. Lentzen, P. Swiatek, A. Forster, K. Urban, W. Laufs, D. Gerthsen, T. Remmele, and A. Rosenauer, *Philos. Mag. Lett.* **74**, 309 (1996).

¹⁸K. Georgsson, N. Carlsson, L. Samuelson, W. Seifert, and L. R. Wallenberg, *Appl. Phys. Lett.* **67**, 2981 (1995).

¹⁹G. D. Lian, J. Yuan, L. M. Brown, G. H. Kim, and D. A. Ritchie, *Appl. Phys. Lett.* **73**, 49 (1998).

²⁰M. Grundmann, O. Stier, and D. Bimberg, *Phys. Rev. B* **52**, 11 969 (1995).

²¹A. Wojs, P. Hawrylak, S. Fafard, and L. Jacak, *Phys. Rev. B* **54**, 5604 (1996).

²²M. F. Ashby and L. M. Brown, *Philos. Mag.* **8**, 1083 (1963); **8**, 1649 (1963).

²³S. Matsumura, M. Toyohara, and Y. Tomokiyo, *Philos. Mag. A* **62**, 653 (1990).

²⁴R. Leon, Y. Kim, C. Jagadish, M. Gal, J. Zou, and D. J. H. Cockayne, *Appl. Phys. Lett.* **69**, 1888 (1996).

²⁵R. Leon, T. J. Senden, Y. Kim, C. Jagadish, and A. Clark, *Phys. Rev. Lett.* **78**, 4942 (1997).

²⁶X. W. Lin, Z. Lilientalweber, J. Washburn, E. R. Weber, A. Sasaki, A. Wakahara, and Y. Nabetani, *J. Vac. Sci. Technol. B* **12**, 2562 (1994).

²⁷J. M. Garcia, G. Medeiros-Ribeiro, K. Schmidt, T. Ngo, J. L. Feng, A. Lorke, J. Kotthaus, and P. M. Petroff, *Appl. Phys. Lett.* **71**, 2014 (1997).

²⁸C. J. Humphreys, *Rep. Prog. Phys.* **42**, 1825 (1979).

²⁹T. Mura, *Micromechanics of Defects in Solids*, 2nd ed. (Martinus Nijhoff, Dordrecht, 1987), p. 167.

³⁰J. S. Blakemore, *J. Appl. Phys.* **53**, R123 (1982).

³¹H. P. Degischer, *Philos. Mag.* **26**, 1137 (1972).